Review

Elka R. Georgieva*

Nanoscale lipid membrane mimetics in spin-labeling and electron paramagnetic resonance spectroscopy studies of protein structure and function

DOI 10.1515/ntrev-2016-0080
Received September 8, 2016; accepted November 18, 2016; previously published online January 23, 2017

Abstract: Cellular membranes and associated proteins play critical physiological roles in organisms from all life kingdoms. In many cases, malfunction of biological membranes triggered by changes in the lipid bilayer properties or membrane protein functional abnormalities lead to severe diseases. To understand in detail the processes that govern the life of cells and to control diseases, one of the major tasks in biological sciences is to learn how the membrane proteins function. To do so, a variety of biochemical and biophysical approaches have been used in molecular studies of membrane protein structure and function on the nanoscale. This review focuses on electron paramagnetic resonance with site-directed nitroxide spin-labeling (SDSL EPR), which is a rapidly expanding and powerful technique reporting on the local protein/spin-label dynamics and on large functionally important structural rearrangements. On the other hand, adequate to nanoscale study membrane mimetics have been developed and used in conjunction with SDSL EPR. Primarily, these mimetics include various liposomes, bicelles, and nanodiscs. This review provides a basic description of the EPR methods, continuous-wave and pulse, applied to spin-labeled proteins, and highlights several representative applications of EPR to liposome-, bicelle-, or nanodisc-reconstituted membrane proteins.

Keywords: bicelles; electron paramagnetic resonance spectroscopy; liposomes; membrane protein structure and function; nanodiscs.

***Corresponding author: Elka R. Georgieva,** Department of Physiology and Biophysics, Weill Cornell Medicine, 1300 York Avenue, New York, NY 10065, USA,
e-mail: erg2013@med.cornell.edu

1 Introduction

Biological membranes are fundamental to the existence of all life-forms, defining cells, organelles, cargo vesicles, and other structures. These biomembranes are highly dynamic lipid bilayer structures that carry tightly regulated protein nanomachinery of great complexity with a large diversity of functions. They actively participate in the cell life cycle, performing their activities in association with proteins that either rest on the membrane surface (peripheral membrane proteins) or reside in the membrane milieu traversing the membrane (integral membrane proteins). Therefore, it is unsurprising that membrane proteins are encoded by a large portion – between 15% and 30% – of an organism's genome [1–3]. They play numerous roles in the central processes of living cells, providing the means for signaling, trafficking, homeostasis, and other functions [4–9].

Membrane proteins are targets of pharmacological interest because some of them are associated with diseases such as cancer, neurodegeneration, endocrine disorders, and ischemia [10–17], and others are the targets for efficient drug delivery [18] or the inhibition of drug efflux [19]. Their roles in immune response and antibiotic resistance are also germane to the development of antiviral and antibacterial agents [3, 20]. Therefore, acquiring detailed knowledge about the structure and function of membrane proteins at the molecular level is of high biomedical importance.

Several biophysical methods have been used to study membrane proteins and their roles in healthy organism physiology and disease processes, and the results have yielded insights into protein system organization, function, and structure at various levels of resolution. These methods primarily include NMR spectroscopy in solution and solid state, and X-ray crystallography, the primary tools for revealing structure at the atomic resolution [7, 21–27]. Electron microscopy, with its wide field of view

and lack of required ensemble measurements other than class averaging, can typically resolve the overall shapes of proteins and their larger assemblies, and it is steadily moving toward even higher nearly atomic level resolution. Therefore, the technique is well-suited for examining micro- and nanoscale heterogeneous systems, thereby allowing the study of membrane protein structure in native environments [28, 29]. Förster (or fluorescence) resonance energy transfer is yet another technique that has been applied successfully to membrane proteins [30–32]. Fluorescence resonance energy transfer and electron paramagnetic resonance (EPR), which are appropriate right at the nanoscale, next to the atomic-scale techniques, are highly effective technologies. EPR has rapidly become a routine method for studying the structure and function of biomolecules. Site-directed spin-labeling (SDSL) EPR, which includes continuous-wave EPR (cw-EPR) and pulse EPR distance measurement, is a particularly powerful approach for investigating membrane proteins under close to native conditions. SDSL EPR provides information on protein structure and dynamics and their changes and the allostery caused by ligand binding, local environment, or functional mutations [33–57].

Despite the advancements of SDSL EPR to study membrane proteins under the native conditions of cell membranes [58–60], most structural and functional studies of membrane proteins are conducted *in vitro* with purified proteins that are either detergent-solubilized or reconstituted into phospholipid-based nanosized membrane mimetics such as lysophospholipid micelles, bicelles, nanodiscs, or liposomes. These membrane mimetics provide, to a varying extent, a native-like environment in terms of membrane fluidity, lipid specificity, hydrophobic thickness matching, and other characteristics.

This review outlines the basic concepts of the EPR techniques applied to nitroxide spin-labeled membrane proteins. It also briefly describes key properties and use of lipidic vesicles, bicelles, and nanodiscs (lipodiscs) for *in vitro* SDSL EPR studies of membrane proteins, and discusses several examples of SDSL EPR structure-function studies of peripheral and transmembrane proteins residing in lipid bilayers.

2 Basic concepts of nitroxide spin-labeling and EPR spectroscopy applied to membrane proteins

EPR spectroscopy applied to spin-labeled membrane proteins is a powerful technique for studying protein dynamics [33–36, 40, 41, 45, 48, 52, 53, 61, 62], self-association and hetero-oligomeric complex formation [37, 39, 51, 57, 58, 63–66], protein location relative to the lipid bilayer [35, 36, 48, 67], and protein structure and function in general [38, 41, 43, 45–47, 49, 53, 68–74]. In this review, only a basic summary of the EPR methods and nitroxide spin-labeling is provided; there are other excellent sources that can provide more detailed descriptions of the EPR spectroscopy as biophysical technique and additional spin labels [40, 52, 62, 75–79].

2.1 Nitroxide spin-labeling

During systematic studies of membrane-bound proteins with SDSL EPR, paramagnetic reporter groups (spin labels) are usually introduced through covalent attachment to the cysteine residues of the polypeptide chain through disulfide or thioester bond formation, as in the case of MTS-, iodoacetamido- or maleimido-linked nitroxide probes [45, 80] (Figure 1). These cysteine residues may be endogenous, but they are commonly introduced at specific positions through site-directed mutagenesis, on the background of a cysteine-less protein.

In some cases, proteins are expressed, purified, and spin-labeled in soluble form and then mixed with

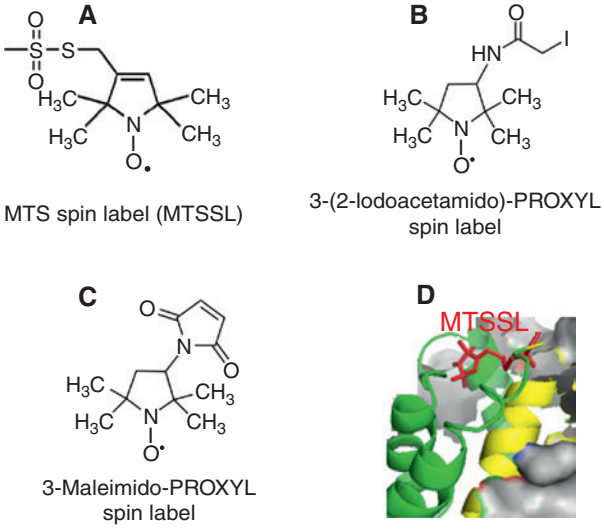

Figure 1: Nitroxide spin-labels commonly used in EPR studies of proteins. (A) MTS spin-label (MTSSL,S-(1-oxyl-2,2,5,5-tetramethyl-2,5-dihydro-1H-pyrrol-3-yl)methyl methanesulfonothioate), which is currently the most widely used spin-label; (B) iodoacetamido-PROXYL spin-label, (C) maleimido-PROXYL spin-label; (D) MTSSL attached to a cysteine residue in a protein polypeptide chain is shown as sticks in red. The side chain of cysteine labeled with MTSSL was produced using MMM software (Polyhach and Jeschke).

membrane mimetic solutions to bind the lipid bilayer surface [48, 68, 69] or integrate deeply into the bilayer, usually traversing it [81] (Figure 2A). *In vivo*, however, most transmembrane proteins are synthesized and concurrently inserted and folded into the cellular membranes by specialized cellular machinery [82]. Therefore, for *in vitro* studies, these proteins are extracted from the native membranes through detergent solubilization, and spin-labeling is performed after protein purification in a detergent solution. The spin-labeled protein is then reconstituted in the lipid bilayer while the detergent is removed (Figure 2B).

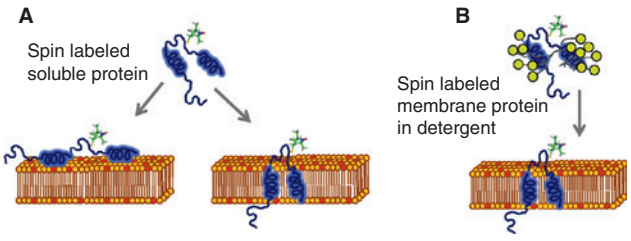

Figure 2: Three cases of protein-membrane association *in vitro*. (A) The protein is expressed and folded in soluble form, but in the presence of lipid membranes it can either bind to the membrane periphery (left) or transverse the membrane (right). Often binding to membrane involves large structural rearangenents. (B) The protein is expressied and folded on the cellular membranes, then it is purified by detergent solubilization and reconstituted in lipid bilayers for *in vitro* functional and structural studies. For EPR studies, in case (A) the proteins are spin-labeled in buffer solution, whereas in (B) the proteins are spin-labeled in detergent-bound form.

2.2 Continuous-wave EPR

The dynamic properties of a typical ^{14}N nitroxide spin label side chain, which depend on both the intrinsic mobility of the spin label and the dynamics of the protein "backbone", can be assessed with cw-EPR by analyzing the EPR spectrum lineshape [83]. For a protein bound to or spanning the lipid membrane, the rate of protein global tumbling has a correlation time (τ_c) of $>10^{-8}$ s, which may be even slower for local dynamics and is well beyond the motional range observed with nitroxide spin-labeling cw-EPR (i.e. $\tau_c \cong 10^{-11} - 10^{-9}$ s; Figure 3A and B). Therefore, for membrane proteins, most of the changes in the spin-label side-chain dynamics caused by alterations in the spin-label local environment, rather than protein backbone motions [84], can be studied by cw-EPR. These are the cases in which significant conformational isomerization may be present – for example, those observed in proteins with spin labels transitioning from more exposed

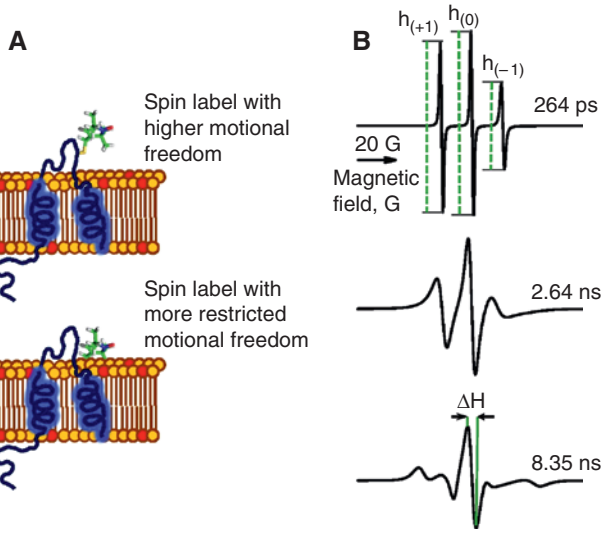

Figure 3: The spin label dynamics and local environment can be monitored by changes in the cw-EPR lineshape. (A) Spin labels introduced in a protein loop regions that are far from the lipid bilayer have higher motional freedom compared to those of spin labels in contact with membrane. (B) Simulated cw-EPR spectra with τ_c of 264 ps, 2.64 ns and 8.35 ns are shown. EPR spectra were simulated using the MultiComponent software of C. Altenbach. The peak-to-peak intensities, $h_{(+1)}$, $h_{(0)}$ and $h_{(-1)}$, of the three lines in the nitroxide spectrum are indicated in the upper panel. The width ΔH of the central line in the nitroxide spin label EPR spectrum is shown in the lower panel. All spectra were scaled to a common value at maximum intensity for clarity of presentation.

and less confined apo states to more occluded and motion-restricted states produced after substrate binding or changes in the local environment [80, 85].

In general, the spin label dynamics in the EPR fast motional regime (i.e. $\tau_c \cong 10^{-11} < 10^{-9}$) can be estimated from the ratio of peak-to-peak intensities of the first and second lines ($h_{(+1)}/h_{(0)}$) in the ^{14}N nitroxide cw-EPR spectrum (Figure 3B, upper panel) [86, 87]. Another coarse approach for quantifying spin-label dynamics is based on the estimated value of the inverse width of the central line of the nitroxide spin-label EPR spectrum ($1/\Delta H$ parameter; Figure 3B, lower panel) [88]. Alternatively, the more comprehensive nonlinear least-squares EPR spectrum analysis [89] yields the diffusion tensor, R, and ordering parameters for spin label motion [90]; thus, yielding τ_c and its dependence on local protein structure.

Another potent cw-EPR-based approach to study the membrane protein structure and function in lipid bilayers relies on solvent accessibility and membrane insertion depth measurements (Figure 4A). This method is based on the relaxation enhancement (mainly affecting spin-lattice relaxation time, T_1) produced by paramagnetic relaxation agents (PRAs) such as oxygen, which partitions

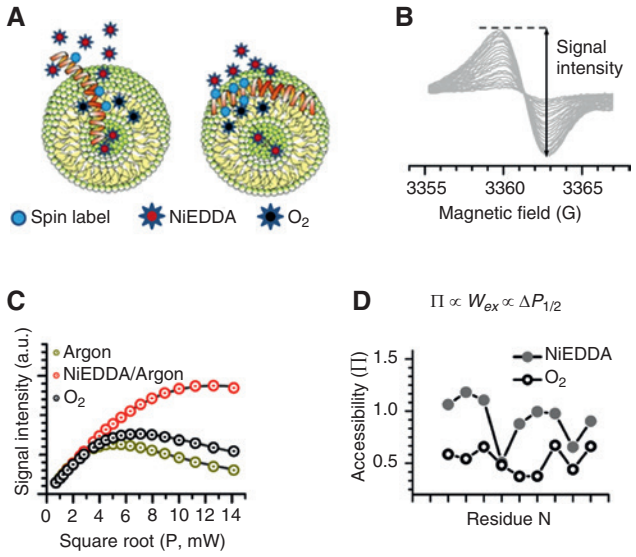

Figure 4: The accessibility to a fast relaxing agent, such as NiEDDA or O_2 can reveal the topology of a membrane protein. (A) A schematic representation of cw-EPR accessibility experiment on membrane protein. Multiple spin-labels are shown to illustrate the proximity to either oxygen or NiEDDA. The actual experiment is conducted on multiple singly spin-labeled protein variants (B) The intensity of central line of ^{14}N nitroxide label increases as a function of applied mw power. (C) Typical saturation curves. The colored circles represent experimental data with and without PRAs. The half saturation parameter $P_{1/2}$ is extracted from fittings of the experimental data. $\Delta P_{1/2}$ is the increase of $P_{1/2}$ in the presence of PRA compared to sample in argon or nitrogen only. (D) Plots of accessibility parameter $\Pi(O_2)$ and Π(NiEDDA) as a function of spin-labeled residue position – the residues with greater $\Pi(O_2)$ are in closer contact with the membrane and vice versa. The accessibilities to PRAs depend on the collision rate and spin-exchange frequency.

predominantly into the lipid bilayer, and a nickel(II)-*N*,*N*1-ethylenediamine-diacetic acid complex (NiEDDA) present only in the aqueous solvent [91, 92]. Commonly, the intensity of the central peak in the EPR spectrum of the ^{14}N nitroxide spin label is measured as a function of the applied microwave (mw) power (Figure 4B). It increases with mw power until saturation is reached at sufficiently high power, i.e. the population difference between the two EPR energy levels becomes progressively smaller and spectral line intensity decreases; also, line broadening occurs in the EPR spectrum. Thus, the maximum EPR line intensity is observed at certain power levels. The position of this maximum can be shifted toward higher mw power through collisions with PRAs, which enhances relaxation through strong spin exchange.

The efficiency of this process depends on the collision rate and Heisenberg exchange frequency, W_{ex}, proportional to the local PRA concentration. For membrane proteins, the relaxation of spin labels attached to residues in solvent-accessible regions is affected by soluble NiEDDA, whereas molecular oxygen has a much greater effect on spin labels residing in the membrane owing to its very high solubility in the hydrophobic core of the lipid bilayer. Thus, in a typical nitroxide label saturation experiment, the saturation curve (i.e. EPR central line intensity vs. applied mw power) is measured under oxygen-free conditions (e.g. in nitrogen or argon), in the presence of oxygen, and finally under anaerobic conditions (argon, nitrogen) in the presence of NiEDDA (Figure 4C). Then, the half-saturation parameter ($P_{1/2}$), which corresponds to the mw power needed to produce an EPR spectrum intensity half that observed in the absence of saturation, is determined. The effect of W_{ex} on $P_{1/2}$ ($\Delta P_{1/2}$) allows the determination of the dimensionless parameter Π (known as the accessibility parameter) for each case (Figure 5D). Finally, the contrast or membrane depth parameter, Φ – defined as $\ln[\Pi(O_2)/\Pi(\text{NiEDDA})]$ – provides the location of the spin-labeled residue with respect to the bilayer.

2.3 Pulse EPR distance measurements and spin counting

At present, the most powerful biophysical EPR method used in membrane protein structural and functional biology is based on nanometer-range distance measurements determined with pulsed dipolar EPR spectroscopy (PDS) applied to doubly spin-labeled (bilabeled) protein molecules or singly spin-labeled subunits comprising protein complexes (Figure 6). PDS measures the strength of the static magnetic dipole-dipole interactions between the electron spins of interacting spin labels. Typically, PDS experiments use nitroxide spin labels and are conducted on frozen solutions at cryogenic temperatures from 50 K to 80 K. To date, the following variants of PDS have mainly been applied to proteins: three-pulse double electron-electron resonance (DEER) [93, 94]; four-pulse DEER [75, 76, 95–97], five-pulse DEER [98], double-quantum coherence [76, 99, 100], and relaxation-induced dipolar modulation enhancement [101–105]. Several other methods have been developed but are rarely used [106, 107] owing to a range of difficult-to-overcome shortcomings.

Currently, the most widely used PDS techniques in biophysical studies is the four-pulse two-frequency DEER spectroscopy (Figure 5) followed by double-quantum coherence EPR [43, 75–77, 96]. They provide direct information on the strength (frequency, ν_{dd}) of the magnetic dipole-dipole interaction between the coupled

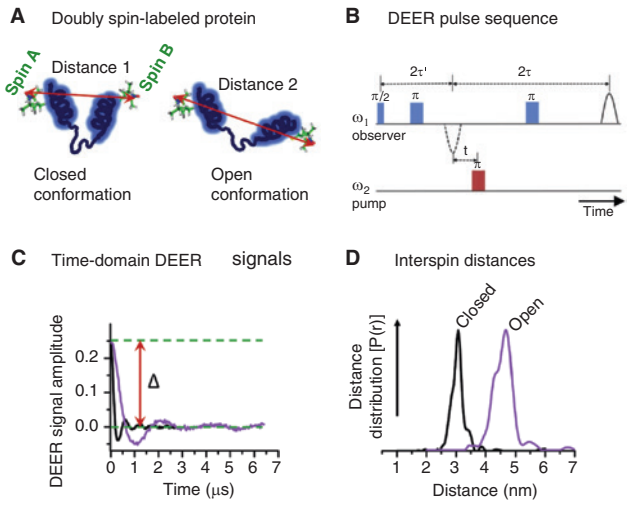

Figure 5: Distance measurements based on the four-pulse DEER experiment. (A) DEER measures distances between pairs of spin labels in protein molecules and complexes. Two conformations of a doubly spin-labeled protein are shown. In frozen solutions the nitroxide spin labels (and the magnetic tensors of their electron spins) have different orientations relative to the external magnetic field, hence leading to broad EPR spectra due to magnetic tensors anisotropy. Consequently, two groups of similarly oriented nitroxides, referred to as "Spins A" and "Spins B" corresponding to different parts of the EPR spectrum can be selected and their dipole-dipole interaction determined by using for example a DEER pulse sequence in order to produce the interspin distance. (B) The most often used four-pulse DEER sequence is shown. In this sequence the three "observer" microwave (mw) pulses are applied to spins A (at mw frequency ω_1) to form a spin-echo, whereas spins B (at mw frequency ω_2) are "pumped" by flipping them with an additional pulse, which does not affect A-spins directly. The dipole-dipole coupling between A and B spins is then recorded by changing the position, *t*, of the pump pulse relative to the static "observer" pulses. The resulting characteristic oscillatory pattern of the amplitude of the spin-echo formed by A-spins gives rise to the "form-factor", *V(t)*, that depends on the strength of dipolar interaction and thereby the distance. (C) Typical time-domain DEER signals (after background correction) recorded with the DEER pulse sequence are shown. These signals are, in general, oscillatory decaying signals with the period of "dipolar" oscillation ~ r^3 (the distance between the spin labels in a protein). For the same spin-labeled residues, DEER signals reflect the interspin distance in each protein conformation, giving generally a range of distances. The modulation depth, Δ, which depends on the number of interacting spins is shown. (D) The distances reconstructed from the DEER signals depicted in (C).

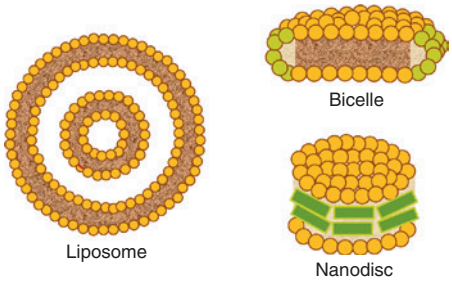

Figure 6: Schematic representation of liposomes, bicelles and nanodiscs used as membrane mimetics in study of membrane proteins structure and function. The liposome shown here has two lipid bilayers. Generally, the mutilamellar liposomes consist of several bilayers, whereas the unilamellar liposomes have only one bilayer. Bicelles have discoidal shape and are formed by mixing lipids with long (orange) and short (green) chains. Nanodiscs are discoidal lipid nanoobjects, which integrity and shape are supported by a belt of two scaffold proteins illustrated in green.

electron spins of the spin labels attached to protein molecules (Figure 5A), hence the distance, because $\nu_{dd} \sim 1/r^3$ (the period of DEER time-domain signal oscillations ~ r^3) (Figure 5C). The following ratio is often used to determine the distance: $\nu_{dd} \equiv \omega_{dd}/2\pi = 52.04/r^3$, with measured ν_{dd} expressed in megahertz and r is in nanometers. An important consideration is that the "raw" DEER signal obtained for a typical sample is contributed by two factors: (1) the intramolecular signal of interest, which contains an inherent constant background, and (2) the decay of intermolecular origin. The intermolecular contribution has to be factored out and the constant background in the intramolecular signal is then removed, thus leaving a pure spin-spin interaction signal (a decaying and generally oscillating time-domain DEER signal as shown in Figure 5C). This procedure is referred to as "background correction." The final time-domain DEER data (and also data produced using other PDS techniques) are processed into interspin distances and distance distributions by using software packages based on Tikhonov regularization or Monte Carlo methods for distance reconstruction [108–110]. The method of maximum entropy [111] can be applied to refine distance distributions obtained with the L-curve Tikhonov regularization approach [108]. Four-pulse DEER and the rest of PDS methods are suitable for measuring spin-spin distances in the range of 1.5 to 8.5 nm [68, 69, 75, 76, 96, 112], with the potential to go beyond 10 nm [98]. However, the accessible distance range depends strongly on the specific system.

Besides distance measurements, DEER can also be used to assess the number of interacting spins within a protein complex. This is based on the modulation depth (Δ) of the DEER signal, which depends on the number of interacting spins as $\Delta(p, N) = 1-(1-p)^{N-1}$, where p is determined by the fraction of spins flipped by the pump pulse, and N is the number of interacting spins in the nanoobject [93, 113–115]. In Figure 6C, Δ appears as the dipolar signal amplitude at the evolution time of zero.

3 Liposomes, bicelles and nanodiscs as membrane mimetics

Liposomes are lipidic nano- and micrometer-sized vesicles consisting of a hydrated lipid bilayer (unilamellar vesicles) or multiple bilayers with onion-like layer morphology (multilamellar vesicles) and filled with aqueous solution (Figure 6, left) [116]. Unilamellar vesicles, which are good mimetics of biological membranes, range in diameter from 20 nm to >1 μm and are further classified as small (20–100 nm), large, (>100 nm), and giant (>1000 nm – i.e. approximately cell size). Multillamellar vesicles usually have diameters of >500 nm. The physical and chemical properties of liposomes have been widely studied for decades, with large efforts devoted to drug delivery [116–118]. However, they have also been used extensively in biochemical and biophysical studies of membrane proteins [119, 120]. Liposomes have the advantage of being close mimetics of biological membranes because they can be made of native as well as synthetic phospholipids, and their size and composition can be controlled. The hydrophobic thickness, fluidity, and lateral pressure of the bilayer [121] can be adjusted by adding cholesterol and selecting lipids with suitable headgroups, polycarbon chain lengths, and degrees of saturation. Therefore, protein reconstitution in liposomes has been widely and successfully used to investigate protein-lipid interactions. Lipid regulation of membrane protein function, membrane protein structure, protein and lipid lateral diffusion, and the formation of protein complexes can all be studied [119, 120].

Bicelles are discoidal lipid bilayered nanostructures composed of short- and long-chain lipids in molar ratios that define their morphology [122] (Figure 6, upper right). Because, unlike liposomes, they lack an aqueous interior, the lipid bilayer and reconstituted proteins are always accessible for soluble protein binding or interacting with ligands. Moreover, these lipid nano-objects provide a true lipid bilayer environment and hydrophobic matching, which are central to protein function. First introduced by Sanders and colleagues [123] as mixtures of 1,2-dimyristoyl-*sn*-glycero-3-phosphocholine (DMPC) and 1,2-dihexanoyl-*sn*-glycero-3-phosphocholine (DHPC), bicelles have been studied extensively, and a range of bicelle sizes and lipid compositions have been used in structural studies of membrane proteins pioneered by NMR spectroscopy [25, 124–126]. Bicelle size can be controlled by changing the molar ratio of long-chain to short-chain lipids. This ratio is known as the q value. One known issue with bicelles is that their sizes change after dilution in aqueous buffers because the fraction of the bicelle-bound and free monomers of the short-chain lipid changes owing to the high critical micelle concentration.

Outside of NMR spectroscopy, bicelles have been used in the crystallization of membrane proteins [127, 128] and for transdermal drug delivery [129]. In EPR spectroscopy, isotropic bicelles with q values of ≤ 2.5 (6) are generally used to ensure uniform distribution and adequate concentration; however, their size must be large enough to accommodate trans- or surface-bound membrane proteins, which require diameters that may reach ≥ 10 nm [66, 68, 69, 130]. Magnetically aligned bicelles of large size have also been used in EPR [131].

Nanodiscs are discoidal nanosized lipid bilayers that lack short-chain lipids and are stabilized with a belt of scaffold protein dimer [132, 133] (Figure 6, lower right). Similar lipid nano-objects, called lipodiscs, are formed by corralling lipids with an annular belt of a copolymer of styrene and maleic acid taken in a molar ratio of 3 : 1 [134–136]. The scaffold proteins or polymers reside at the periphery of the bilayer, where they take the place of short-chain lipids. Similar to bicelles, nanodiscs are highly soluble in aqueous buffers but have the advantage of maintaining their sizes after dilution. Therefore, nanodiscs can be used in a wide range of concentrations, which makes them conveniently applicable to studies of membrane proteins that use multiple biophysical techniques, including NMR [125, 137], surface plasmon resonance [138], X-ray crystallography [139], and electron microscopy [140, 141]. The number of EPR studies of nanodisc-reconstituted membrane proteins has grown significantly in recent years [47, 134, 142–145].

EPR spectroscopy of spin-labeled proteins – in particular, distance measurements based on pulse EPR methods – benefit from the use of bicelles and nanodiscs because experiments with much higher sensitivity are possible owing to the capacity to achieve high concentrations of isolated protein molecules. This is not feasible with liposome-reconstituted proteins in which the local concentration is relatively high because of protein confinement to the liposome surface that causes crowding. Furthermore, compared with liposomes, the spin labels in bicelles and nanodiscs usually have longer phase memory relaxation times (T_m), which allows the recording of pulse EPR signals to much longer dipolar evolution times (i.e. much longer interval for stepping-out the pump pulse in Figure 5B that is the distance between the second and the third observer pulses), thereby leading to better-resolved distances and more accurate distance distributions [47, 68, 69, 142]. On the contrary, some studies have shown that

the lipid dynamics and phase transitions in both bicelles and nanodiscs/lipodiscs are affected by their finite size [134, 146]. Thus, an increase in lateral stress in a small patch of bilayer can affect protein structure and function.

4 Examples of EPR studies of membrane proteins in liposomes, bicelles, and nanodiscs

4.1 Structure and function of liposome- and bicelle-bound peripheral membrane proteins

Human alpha-synuclein (αS) is a highly abundant protein in the neurons of the central nervous system that associates with synaptic vesicles and may have cellular roles in synaptic vesicle trafficking and neurotransmitter release [147, 148]. αS has been linked to several neurodegenerative disorders – for example, αS amyloid deposits are a hallmark of Parkinson's disease [147, 148]. Thus, comprehensive study of the lipid-bound structure of αS is critical to understanding the physiological role and function of this protein and may provide insights into the mechanisms leading to its malfunction. αS contains 140 amino acids and can be divided into the positively charged N-terminal domain, uncharged middle region composed of residues 61 to 95 (also called the nonamyloid component, NAC); and the highly acidic C-terminal domain. Early spectroscopic studies have shown that this protein undergoes a remarkable conformational transformation – from being unstructured in solution to having a distinct structure with high helical content when bound to membrane mimetics [149–151].

In the context of membranes, solution NMR provided the first high-resolution structure of αS [152], although it was limited to detergent micelles, which are not fully representative of the curvature, headgroups, local and collective dynamics, lateral pressure, and other features of lipid bilayers. The NMR structure showed that the N-terminal domain and NAC region of αS (i.e. residues 3–92) associated with the detergent by forming a U-shaped helix interrupted by an ordered linker at residues 38 to 44, whereas the C-terminal domain remained free and largely unstructured [152]. This structure was later confirmed comprehensively with long-range DEER distance measurements carried out on micelle-bound αS [153]. Furthermore, significant information on how this protein interacts with native membrane was obtained through several outstanding EPR studies on liposome- and bicelle-bound spin-labeled αS. These studies used both cw-EPR and DEER spectroscopy [68, 69, 154–159]. Initially, cw-EPR was applied to elucidate the structure of membrane-bound αS [154]. EPR spectra of proteins with single spin-labeled residues spanning the entire sequence were recorded in their free states in solution and bound to small unilamellar vesicles composed of a 7 : 3 ratio of 1-palmitoyl-2-oleoyl-*sn*-glycero-3-phosphocholine (POPC) and 1-palmitoyl-2-oleoyl-*sn*-glycero-3-phospho-L-serine (POPS) lipids and average size of 30 to 40 nm. The conformational change, which takes place when the proteins interact with the phospholipid membrane, was detected with cw-EPR in the N-terminal domain and NAC as evidenced by EPR spectral broadening indicative of much slower protein and spin label dynamics, whereas only minor spectral changes were noticed for the highly acidic C-terminal domain [154].

In the same study, the secondary structure of the membrane-associated region of αS was determined by measuring the cw-EPR spectra mw power saturation of spin labels placed at various spin label sites, which granted access to the strong relaxing agents oxygen and NiEDDA. The respective accessibility parameters, $\Pi(O_2)$ and Π(NiEDDA) [36], showed periodic patterns characteristic of an alpha-helix. The narrow range of contrast parameter (Φ) values obtained for the residues on the same side of the helix (Figure 7) and the ratio of the Φ values of the protein to those of the spin-labeled lipids suggested that αS residues do not reach the membrane hydrophobic core but rather associate with the membrane surface and form an amphipathic helix. Furthermore, the results showed that the residues, which are in contact with the membrane, participate in hydrophobic and possibly electrostatic interactions with negatively charged lipid headgroups [154, 155]. Importantly, the residues in the linker region – i.e. residues 42–44, were significantly more ordered than would be expected in the micelle-bound structure, which suggested that the structure of this region might also tend to be helical [154].

Unambiguous support for this prediction and the first direct experimental evidence that micelle- and membrane-bound structures of αS have vastly different spatial organizations was obtained with DEER studies of wild-type αS and its mutants implicated in familial forms of Parkinson's disease [68, 69] (Figure 8). These studies used unilamellar vesicles and isotropic bicelles with a high content of negatively charged phospholipids (liposomes of either POPC/POPA (1-palmitoyl-2-oleoyl-*sn*-glycero-3-phosphate) or DMPC/DMPG, and bicelles of DMPC/DMPG/DHPC with a q value of 2.6). A series of DEER measurements of doubly

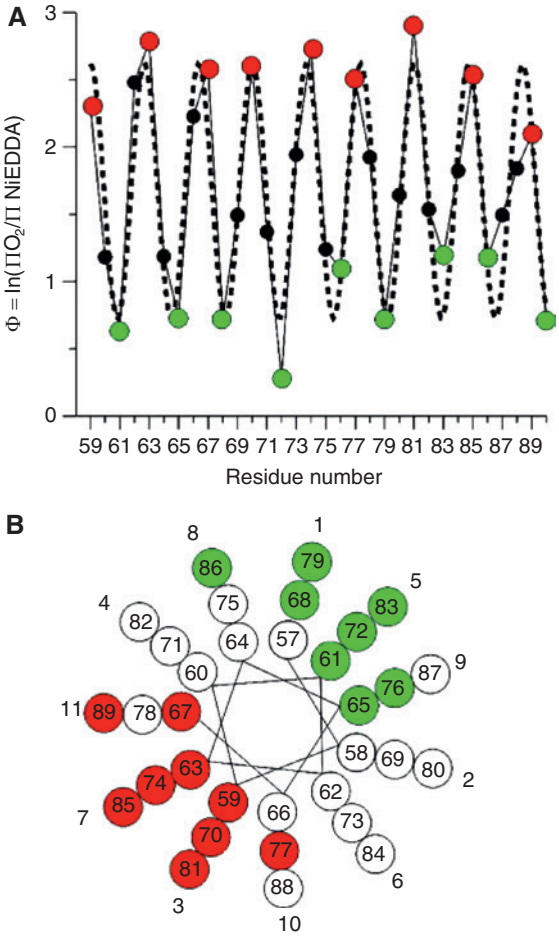

Figure 7: Secondary structure and topology of R1-labeled α-synuclein. (A) The ratios of the O_2 and NiEDDA accessibilities are summarized by the contrast parameter Φ. High Φ values indicate lipid-exposed sites (red) whereas low Φ values indicate solvent-exposed sites (green). The dashed line indicates the best fit to a cosine function resulting in a periodicity of 3.67 aa per turn. (B) When residues are plotted on a helical wheel with a periodicity of 3.67 aa per turn, lipid-exposed sites (red) are on one side whereas solvent-exposed sites (green) lie on the opposite side. White circles denote residues with Φ values that are neither maxima nor minima. The figure was reprinted from Jao CC, Der-Sarkissian A, Chen J, Langen R. *Proc. Natl. Acad. Sci. USA.* 2004, 101, 8331–8336. Copyright (2004) National Academy of Sciences, USA, and the kind agreement of Dr. Ralf Langen.

spin-labeled αS mutants covering distances ranging from ~2 nm to nearly 9 nm established that αS and its mutants adopt an extended helix conformation when bound to lipid membranes if the surface area can accommodate a helix longer than 90 amino acids [68, 69]. Importantly, the protein-to-lipid molar ratios were optimized for liposomes and bicelles in these studies to ensure correct assignment of the intermolecular distances. Thus, in the case of liposomes, the lipid-to-protein molar ratio was 1 : 1000 or greater to minimize lateral contacts (nonspecific aggregation), and in the case of bicelles, the ratio was selected to ensure an average of no more than one protein molecule per bicelle. Furthermore, deuterated lipids (DMPC-d_{67}/DMPG-d_{54}) and 70% deuterated protein mutants were used to allow the measurement of long distances of up to 8.5 nm. This study was the first to use deuterated membrane proteins (and proteins in general) for long-distance measurements with DEER.

Several other EPR-based studies have helped illuminate αS-membrane interactions. The results showed that the straight extended helix is not the only αS structure observed on lipid membranes. A U-shaped conformation [156] similar to that found in NMR studies of micelles [152] is also observed. In addition, αS forms aggregates of monomers in broken helix conformations on lipid membranes [157]. Overall, these nanoscale EPR studies with lipid vesicles and isotropic bicelles have established that αS adopts multiple membrane-associated conformations, and this structural plasticity is now believed to be a prerequisite for supporting its physiological functions.

Recently, the structure of the microtubule-binding domain of human tau protein was thoroughly characterized with liposomes in the same type of pulse/cw-EPR study [48] that proved so successful for αS. cw-EPR accessibility scans provided structural information at the secondary structure level, whereas long-range distance measurements obtained with DEER reported on the tertiary structure of tau at the membrane surface. The results showed that, upon interaction with the membrane surface, microtubule-binding domain folds into short amphipathic helices connected by relatively flexible linkers. No tau aggregation was detected under these experimental conditions, however. This study was one of the first to investigate the interaction of tau and biological membranes. It was shown that tau undergoes a considerable structural transition from a disordered state in solution to a highly folded state in lipid. Although the primary role of tau is microtubule binding and stabilizing [160, 161], it also interacts with biological membranes in the cell [162]. Other *in vitro* studies have indicated the possibility of tau misfolding and aggregation on lipid bilayers [163]. Therefore, understanding tau-lipid interactions might be key to elucidating its physiological functions and the mechanisms of tau misfolding that lead to neurodegeneration [164].

4.2 Structure and function of membrane transporters in liposomes and nanodiscs

During the last decade, EPR spectroscopy has been applied extensively to the study of membrane transporter

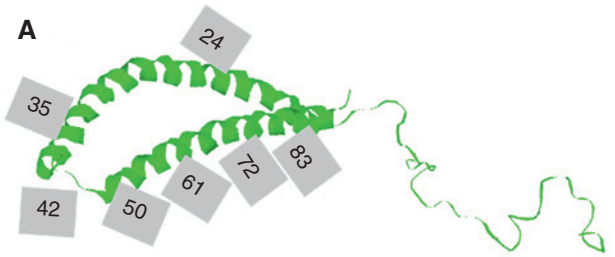

B

Labeled sites	Distances (nm)	
	Experimental DEER	α-helix Rise 0.15 nm
50/72	3.5	3.3
20/42	3.3	3.3
42/61	3.6	2.9
35/50	2.0	2.3
24/61	5.5(6)	5.55
24/72	6.9	7.2
24/83	8.7	8.85

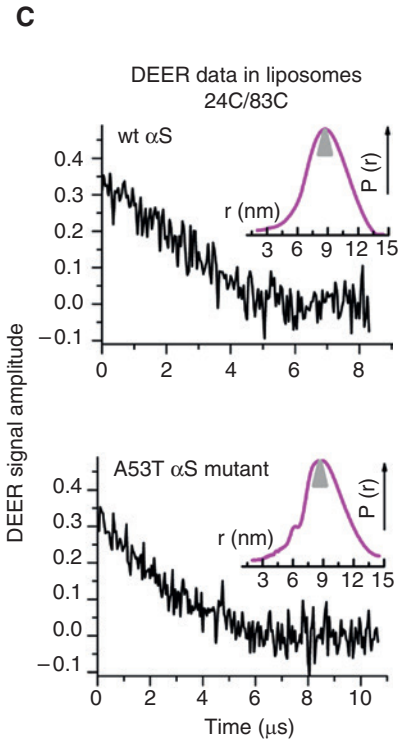

Figure 8: DEER-derived distances suggest single-extended helix conformation of lipid-bound αS (Ref. 68 and 69). (A) Cartoon of micelle-bound αS determined by NMR (PDB 1XQ8). Shown are the approximate positions of spin-labeled αS residues used for DEER distance measurement in wt protein and familial Parkinson's disease (PD) mutants (A30P, E46K, A53T). (B) The DEER-derived distances for liposome-bound multiple double spin-labeled mutants in wt αS agree well with those expected for an extended alpha helix, but not the U-shaped conformation. The distances between the residues within the same segment of the broken helix are shown in black while those between different segments are in blue. Similar distances were measured in context of bicelles, and for all αS variants (wt and PD mutants). (C) The background-corrected DEER time-domain data (black) and reconstructed distances (magenta) for spin-labeled-residues 24C/83C in wt αS and A53T mutant. Very long distances of up to ca. 9 nm were obtained.

and channel structures and functions under native-like conditions in a lipid bilayer [33, 38, 39, 41, 46, 49, 57, 59, 66, 70, 72, 73, 85, 130, 143, 145]. Two EPR studies of membrane transporters – namely, the sodium/aspartate symporter Glt_{Ph} [57, 165] residing in liposomes and the multidrug transporter LmrP inserted into nanodiscs [145] – are highlighted here.

The homotrimeric integral membrane protein Glt_{Ph} is a homolog of mammalian plasma membrane glutamate transporters. For more than a decade, Glt_{Ph} has been a major source of transporter structural information provided primarily by X-ray crystallographic studies in detergent micelles, which are typically used with this class of proteins [32, 166–169]. Each protomer in Glt_{Ph} comprises a stable trimerization domain and a highly dynamic transport domain, which harbors the substrate-binding site and isomerizes between outward- and inward-facing conformations [167, 168]. The first insights into the mode of structure-function coupling for this transporter in solution and, most importantly, in lipid membranes were provided through EPR spectroscopy studies [57, 165, 170]. An extensive DEER study of 10 spin-labeled Glt_{Ph} mutants showed that protomers within the Glt_{Ph} trimer adopt outward and inward conformations with almost equal probability under both ligand and nonligand conditions, although the binding of substrate or inhibitor slightly favors the outwardly open state (open to the periplasm) (Figure 9) [57]. This study concluded that these global Glt_{Ph} conformations have similar energies and independently functioning subunits, and these findings were buttressed by an independent DEER study of the same protein that used different spin-labeled positions and a DOPE/DOPC/DOPG [1,2-dioleoyl-*sn*-glycero-3-phosphoethanolamine/1,2-dioleoyl-*sn*-glycero-3-phosphocholine/1,2-dioleoyl-*sn*-glycero-3-phospho-(1′-rac-glycerol)] lipid environment [165]. Both studies were extremely challenging in that they pushed the limits of measurable distances with the DEER method in large membrane-residing proteins. Thus, distances greater than 6 nm were measured. Importantly, the capacity of DEER to study proteins under near-native

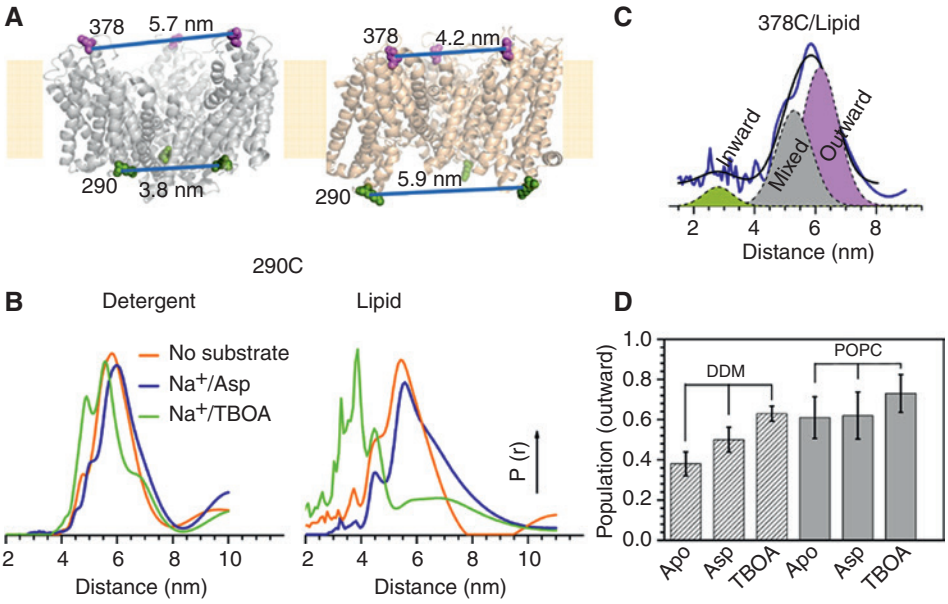

Figure 9: In detergent solution and in lipid membranes GltPh protomers occupy outward and inward facing conformations with almost equal probability (Ref. 57). (A) Glt_{Ph} homotrimer in outward (PDB 2NWX) and inward (PDB 3KBC) facing states is shown. Indicated are the position of residue 290 (green) and 378 (magenta) used for spin-labeling and expected C_β-C_β distances based on crystal structures. (B) DEER-derived distances for spin-labeled residue 290C in detergent (left) and in POPC lipid (right) are shown. Broad distance distributions covering distances expected for both outward and inward facing state were obtained. (C) Experimental distance distributions were fitted to a sum of three Gaussians whose weights are defined by the probability of a protomer to occupy outward, inward, or mixed (inward and -outward) state; thus the populations of the two global conformations (i.e. these open to periplasm or cytoplasm) were determined – as demonstrated for the residue 378C in the case of lipid. (D) Based on these analyses, it was established that Glt_{Ph} protomers sample outward and inward facing conformations with almost equal probability regardless of the presence of substrate (Na^+/Asp) or inhibitor (Na^+/TBOA).

conditions and the unique DEER-based findings of these studies made considerable contributions to the concept of a novel functional mechanism – referred to as an "elevator" mechanism – for membrane transporters [171].

DEER spectroscopy has been used to study proteins in nanodiscs as well. LmrP, a multidrug transporter belonging to the major facilitator superfamily that uses proton translocation down a transmembrane gradient to power the transport of structurally dissimilar substrates, has recently been studied with this technique [145]. Inter-spin distances in several doubly spin-labeled mutants of LmrP monomers located on the extracellular or intracellular ends of transmembrane helices involved in substrate translocation were measured under various ligand and pH conditions (pH 4.5–8.5) as well as in bilayers with various lipid compositions.

The studies found that the binding of substrate with transporters reconstituted in nanodiscs of *Escherichia coli* polar lipids favors the outward-facing conformation over the entire pH range. This conformational distribution differs from that in detergent (Figure 10), thus highlighting the importance of the lipid environment. To further detail the functional role of lipids, spin-labeled LmrP mutants were reconstituted in nanodiscs made of lipids with various polycarbon chains or headgroups, and particularly the methylation state of DOPE. Although the influence of polycarbon chains on the DEER-derived distance distributions was marginal, the degree of DOPE methylation had a strong pH-dependent effect on this distribution and, in turn, on the population of outward- and inward-facing states. DOPE methylation thus stabilized the outward-open conformation, particularly at high pH. Cardiolipin also had a pronounced effect on LmrP conformational states. Collectively, the findings from this study suggest a key role for protein-lipid interactions in the regulation of the ion- and substrate-dependent conformational dynamics of the LmrP transporter, and these interactions may be relevant to other secondary transporters as well [145].

4.3 Assembly of membrane proteins in liposomes

Understanding the assembly mechanisms of functional oligomeric membrane proteins in the lipid bilayer is an

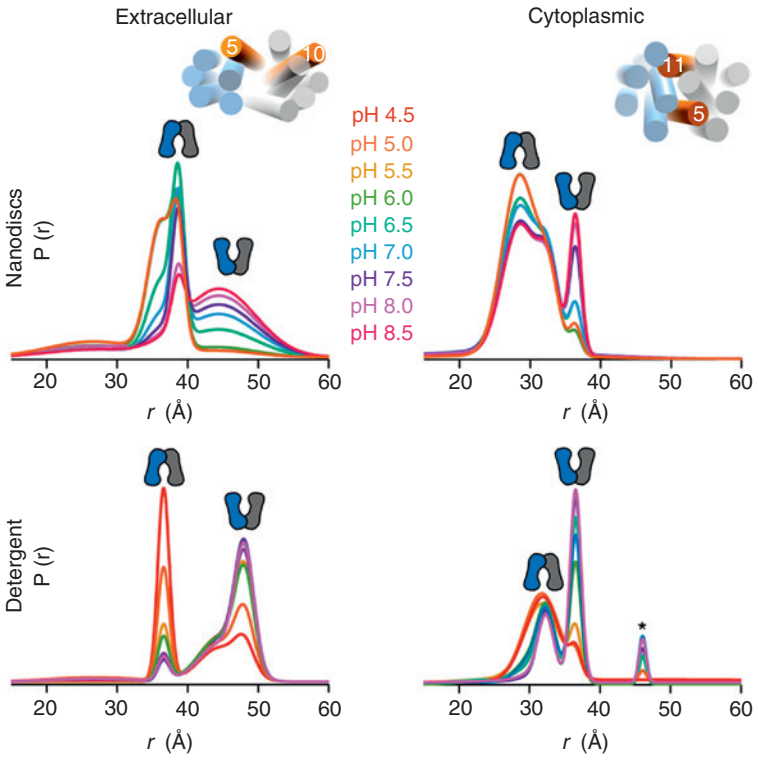

Figure 10: DEER distance distributions of the 160R1–310R1 and the 137R1–349R1 pairs, used as extracellular (left) and cytoplasmic (right) reporters, respectively, in the multidrug transporter LmrP. Top, mutants reconstituted in E. coli polar lipid nanodiscs, at pH values ranging from pH 5 to pH 8.5 in 0.5-unit increments. Bottom, mutants in detergent micelles, at pH values ranging from pH 4.5 to pH 8 in 0.5-unit increments. Asterisks denote peaks resulting from partial aggregation observed in some samples after concentration. Reprinted by permission from Macmillan Publishers Ltd: [Nat Struct Mol Biol] (Martens C, Stein RA, Masureel M, Roth A, Mishra S, Dawaliby R, Konijnenberg A, Sobott F, Govaerts C, McHaourab HS. *Nat. Struct. Mol. Biol.* 2016, 23, 744–751), copyright (2016) and the kind agreement of Dr. Hassane Mchaourab. In this figure R1 denotes the cysteine residue with disulfide-linked MTSSL.

important goal in biology. Achieving this goal is rather challenging, however, owing to the limitations of available biophysical and biochemical experimental methods. In this respect, DEER spectroscopy is a particularly useful technique because it can assess protein complex formation regardless of subunit or whole-protein size. Typically, protein subunits residing in lipid bilayers are singly spin-labeled to determine their complex formation, a method that relies on so-called spin-counting based on the DEER modulation depth (Δ), which depends on the number of interacting spins in the nano-object (see Pulse EPR distance measurements and spin counting) [113–115]. Thus, sufficiently separated singly labeled monomers produce no distinct DEER signal, but nanometer-sized dimers and higher-order oligomers give rise to distinct DEER signals with Δ values that increase with increases in oligomerization order.

This advantage of DEER spectroscopy was used to assess the pH-dependent dimerization of an NhaA Na^+/H^+ antiporter of *Escherichia coli* in proteoliposomes [37]. The observed increase in DEER modulation depth after pH increase from 5.8 to 8 indicated that the functional form of NhaA is a dimer. DEER measurements were also performed on singly spin-labeled synaptobrevin in liposomes, which established that the protein had a predominantly dimeric state [65]. DEER experiments on colicin A monomers inserted into liposomes and intact *E. coli* cells demonstrated that protein self-assembly occurs on the membrane, thereby advancing knowledge of the functional state of this toxin [58]. DEER spectroscopy was also used to study the oligomer formation of liposome-bound Bax protein, which plays a central role in the mitochondrial pathway of apoptosis [63]. The observed DEER signals showed that on membranes, the pore-forming active Bax assembles into dimers. Recently, DEER data were used to characterize Snf7, a subunit of the ESCRT-III complex that is active in remodeling membranes in higher organisms through a mechanism that uses protofilaments formed on the liposome surface [172]. The results showed that Snf7 assembles into spiraling, membrane-sculpting filaments that are scaffolds with ~30 Å lattice periods produced through the

stacking of Snf7 units in open conformation representing the active state of this protein.

Spin-counting based on DEER modulation depth was used recently to characterize in detail the assembly path of the transmembrane domain of protein M2 from influenza A virus [51, 56]. M2 forms tetramers (Figure 11A), which function as proton channels in the acidic environment of host cell endosomes [173]. The peptide $M2TMD_{21–49}$, the core of M2, was spin-labeled for DEER measurements at position L46C and reconstituted in DOPC/POPS (1-palmitoyl-2-oleoyl-*sn*-glycero-3-phospho-L-serine) multilamellar liposomes at peptide-to-lipid molar ratios ranging broadly from 1 : 18,800 to 1 : 160 (Figure 11B). The results showed that increases in Δ do not correspond to a simple monomer-to-tetramer assembly; instead, tetramer formation is preceded by a stable intermediate dimer formation (Figure 11C). The outcome was similar at pH 5.5, in which the proton channel is activated, and at pH 8, in which the channel is in a resting state. Thus, a cascade mechanism –that is, monomer ↔ dimer ↔ tetramer – was proposed for this protein assembly in lipid environments [51]. The extracted equilibrium constants for the monomer ↔ dimer and dimer ↔ tetramer transformations suggested a much stronger dimer intermediate and a weaker tetramer.

The study also showed that in thinner membranes of 1,2-dilauroyl-*sn*-glycero-3-phosphocholine/1,2-dilauroyl-*sn*-glycero-3-phospho-L-serine, in which the hydrophobic thickness does not match the length of the M2TMD helix, $M2TMD_{21–49}$ assembles much less efficiently, most likely as a result of hydrophobic mismatch energy penalties [56]. Importantly, for samples with the same peptide-to-lipid molar ratio, increased Δ's were observed upon binding of the anti-influenza drug amantadine at pH 5.5 [56]. The equilibrium analysis showed that the tetramer species become much more stable in the presence of amantadine compared with nonamantadine conditions. These extensive studies on $M2TMD_{21–49}$ assembly under various pH, lipid, and drug conditions [51, 56] are excellent demonstrations of the capacity of the DEER method in studies of complex membrane protein assemblies and conformational equilibria in near-native environments.

5 Conclusions

Coupling advanced lipid nanotechnologies with SDSL EPR spectroscopy is a powerful approach to study functional mechanisms of membrane proteins at the molecular level under native-like conditions. Modern EPR spectroscopy, particularly its advanced pulsed versions, has developed approaches to meet the needs of membrane structural and functional biology, leading to an explosive growth and great diversity of biophysical applications. Importantly, EPR could be applied to a wide range of membrane protein systems in a variety of environments. Virtually no restrictions are imposed on the protein size and lipid membrane morphology.

This short review outlines the properties of several nanostructured membrane mimetics widely used as membrane protein hosts for *in vitro* studies, and it provides the basic concepts of nitroxide spin-labeling and the most used EPR techniques. The featured examples are among many recent successful studies of membrane proteins, demonstrating the great capacity of lipid nanotechnologies and EPR spectroscopy to uncover important physiological properties of proteins and their disease-linked abnormalities.

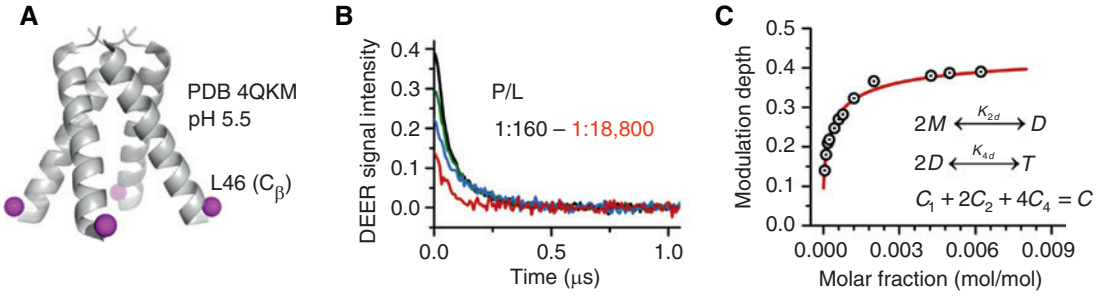

Figure 11: M2 transmembrane domain assembles via a dimer intermediate (Ref. [51]). (A) Tetramer of M2 transmembrane helices at pH 5.5. L46C residue was spin-labeled for DEER study. (B) Background-corrected DEER signals for peptide-to-lipid molar ratios (P/L) ranging from 1 : 160 to 1 : 18,800. The DEER modulation depth strongly depends on P/L in the range from 1 : 18,800 to 1 : 160. Higher order oligomers are progressively more populated as P/L increases. Only selected data are shown for clarity. (C) The fitting of DEER modulation depth values for multiple P/Ls revealed a cascade mechanism of M2TMD assembly, that is monomer(M) ↔ dimer(D) ↔ teramer(T). The equilibrium constants for the 2M ↔ D and 2D ↔ T were obtained. In the figure, C_1, C_2 and C_4 are the concentrations of monomer, dimer and tetramer, respectively. All data shown are at pH 5.5.

Acknowledgments: E.R. Georgieva gratefully acknowledges Dr. Peter Borbat and Dr. Olga Boudker for critical reading of the manuscript and for insightful discussions. The reviewers are acknowledged for their helpful comments. This work was partially supported by NINDS grants R01NS064357 and R37NS085318.

References

[1] Liu J, Rost B. Comparing function and structure between entire proteomes. *Protein Sci*. 2001, 10, 1970–1979.
[2] Mitaku S, Ono M, Hirokawa T, Boon-Chieng S, Sonoyama M. Proportion of membrane proteins in proteomes of 15 single-cell organisms analyzed by the SOSUI prediction system. *Biophys. Chem*. 1999, 82, 165–171.
[3] Poetsch A, Wolters D. Bacterial membrane proteomics. *Proteomics* 2008, 8, 4100–4122.
[4] Hurley JH, Misra S. Signaling and subcellular targeting by membrane-binding domains. *Annu. Rev. Biophys. Biomol. Struct*. 2000, 29, 49–79.
[5] Delcour AH. Solute uptake through general porins. *Front. Biosci*. 2003, 8, d1055–1071.
[6] Busch W, Saier MH Jr. The transporter classification (TC) system, 2002. *Crit. Rev. Biochem. Mol. Biol*. 2002, 37, 287–337.
[7] Gouaux E, Mackinnon R. Principles of selective ion transport in channels and pumps. *Science*. 2005, 310, 1461–1465.
[8] White JM. Viral and cellular membrane fusion proteins. *Annu. Rev. Physiol*. 1990, 52, 675–697.
[9] Cretel E, Pierres A, Benoliel AM, Bongrand P. How cells feel their environment: a focus on early dynamic events. *Cell. Mol. Bioeng*. 2008, 1, 5–14.
[10] Lund R, Leth-Larsen R, Jensen ON, Ditzel HJ. Efficient isolation and quantitative proteomic analysis of cancer cell plasma membrane proteins for identification of metastasis-associated cell surface markers. *J. Proteome Res*. 2009, 8, 3078–3090.
[11] Leth-Larsen R, Lund R, Hansen HV, Laenkholm AV, Tarin D, Jensen ON, Ditzel HJ. Metastasis-related plasma membrane proteins of human breast cancer cells identified by comparative quantitative mass spectrometry. *Mol. Cell. Proteomics*. 2009, 8, 1436–1449.
[12] Cookson MR. Alpha-Synuclein and neuronal cell death. *Mol. Neurodegener*. 2009, 4, 9.
[13] Danbolt NC. Glutamate uptake. *Prog. Neurobiol*. 2001, 65, 1–105.
[14] Goedert M, Jakes R. Mutations causing neurodegenerative tauopathies. *Biochim. Biophys. Acta*. 2005, 1739, 240–250.
[15] Kanai Y, Hediger MA. The glutamate and neutral amino acid transporter family: physiological and pharmacological implications. *Eur. J. Pharmacol*. 2003, 479, 237–247.
[16] Matherly LH, Hou Z, Deng Y. Human reduced folate carrier: translation of basic biology to cancer etiology and therapy. *Cancer Metastasis Rev*. 2007, 26, 111–128.
[17] Vassart G, Costagliola S. G protein-coupled receptors: mutations and endocrine diseases. *Nat. Rev. Endocrinol*. 2011, 7, 362–372.
[18] Giacomini KM, Huang SM, Tweedie DJ, Benet LZ, Brouwer KL, Chu X, Dahlin A, Evers R, Fischer V, Hillgren KM, Hoffmaster KA, Ishikawa T, Keppler D, Kim RB, Lee CA, Niemi M, Polli JW, Sugiyama Y, Swaan PW, Ware JA, Wright SH, Yee SW, Zamek-Gliszczynski MJ, Zhang L. Membrane transporters in drug development. *Nat. Rev. Drug Discov*. 2010, 9, 215–236.
[19] Shukla S, Wu CP, Ambudkar SV. Development of inhibitors of ATP-binding cassette drug transporters: present status and challenges. *Expert Opin. Drug Metab. Toxicol*. 2008, 4, 205–223.
[20] Ramanan P, Shabman RS, Brown CS, Amarasinghe GK, Basler CF, Leung DW. Filoviral immune evasion mechanisms. *Viruses* 2011, 3, 1634–1649.
[21] Montelione GT. The protein structure initiative: achievements and visions for the future. *F1000 Biol. Rep*. 2012, 4, 7.
[22] Hong M, Zhang Y, Hu F. Membrane protein structure and dynamics from NMR spectroscopy. *Annu. Rev. Phys. Chem*. 2012, 63, 1–24.
[23] Boudker O, Verdon G. Structural perspectives on secondary active transporters. *Trends Pharmacol. Sci*. 2010, 31, 418–426.
[24] Caffrey M. Membrane protein crystallization. *J. Struct. Biol*. 2003, 142, 108–132.
[25] Warschawski DE, Arnold AA, Beaugrand M, Gravel A, Chartrand E, Marcotte I. Choosing membrane mimetics for NMR structural studies of transmembrane proteins. *Biochim. Biophys. Acta*. 2011, 1808, 1957–1974.
[26] Deniaud A, Moiseeva E, Gordeliy V, Pebay-Peyroula E. Crystallography of membrane proteins: from crystallization to structure. *Methods Mol. Biol*. 2010, 654, 79–103.
[27] Opella SJ, Marassi FM. Structure determination of membrane proteins by NMR spectroscopy. *Chem. Rev*. 2004, 104, 3587–3606.
[28] Wisedchaisri G, Reichow SL, Gonen T. Advances in structural and functional analysis of membrane proteins by electron crystallography. *Structure* 2011, 19, 1381–1393.
[29] Muller DJ, Wu N, Palczewski K. Vertebrate membrane proteins: structure, function, and insights from biophysical approaches. *Pharmacol. Rev*. 2008, 60, 43–78.
[30] Taraska JW. Mapping membrane protein structure with fluorescence. *Curr. Opin. Struct. Biol*. 2012, 22, 507–513.
[31] Loura LM, Prieto M. FRET in membrane biophysics: an overview. *Front. Physiol*. 2011, 2, 82.
[32] Akyuz N, Georgieva ER, Zhou Z, Stolzenberg S, Cuendet MA, Khelashvili G, Altman RB, Terry DS, Freed JH, Weinstein H, Boudker O, Blanchard SC. Transport domain unlocking sets the uptake rate of an aspartate transporter. *Nature*. 2015, 518, 68–73.
[33] Yilmaz D, Dimitrova AI, Walko M, Kocer A. Study of light-induced MscL gating by EPR spectroscopy. *Eur. Biophys. J*. 2015, 44, 557–565.
[34] Sahu ID, Lorigan GA. Biophysical EPR studies applied to membrane proteins. *J. Phys. Chem. Biophys*. 2015, 5, 188.
[35] Altenbach C, Flitsch SL, Khorana HG, Hubbell WL. Structural studies on transmembrane proteins. 2. Spin labeling of bacteriorhodopsin mutants at unique cysteines. *Biochemistry* 1989, 28, 7806–7812.
[36] Altenbach C, Marti T, Khorana HG, Hubbell WL. Transmembrane protein structure: spin labeling of bacteriorhodopsin mutants. *Science*. 1990, 248, 1088–1092.
[37] Hilger D, Jung H, Padan E, Wegener C, Vogel KP, Steinhoff HJ, Jeschke G. Assessing oligomerization of membrane proteins by four-pulse DEER: pH-dependent dimerization of NhaA Na+/H+ antiporter of *E. coli*. *Biophys. J*. 2005, 89, 1328–1338.

[38] Borbat PP, Surendhran K, Bortolus M, Zou P, Freed JH, Mchaourab HS. Conformational motion of the ABC transporter MsbA induced by ATP hydrolysis. *PLoS Biol*. 2007, 5, e271.
[39] Hilger D, Polyhach Y, Padan E, Jung H, Jeschke G. High-resolution structure of a Na+/H+ antiporter dimer obtained by pulsed electron paramagnetic resonance distance measurements. *Biophys. J*. 2007, 93, 3675–3683.
[40] Klug CS, Feix JB. Methods and applications of site-directed spin labeling EPR spectroscopy. *Methods Cell. Biol*. 2008, 84, 617–658.
[41] Claxton DP, Quick M, Shi L, de Carvalho FD, Weinstein H, Javitch JA, Mchaourab HS. Ion/substrate-dependent conformational dynamics of a bacterial homolog of neurotransmitter:sodium symporters. *Nat. Struct. Mol. Biol*. 2010, 17, 822–829.
[42] McCoy J, Hubbell WL. High-pressure EPR reveals conformational equilibria and volumetric properties of spin-labeled proteins. *Proc. Natl. Acad. Sci. USA*. 2011, 108, 1331–1336.
[43] Mchaourab HS, Steed PR, Kazmier K. Toward the fourth dimension of membrane protein structure: insight into dynamics from spin-labeling EPR spectroscopy. *Structure*. 2011, 19, 1549–1561.
[44] Bhatnagar J, Sircar R, Borbat PP, Freed JH, Crane BR. Self-association of the histidine kinase CheA as studied by pulsed dipolar ESR spectroscopy. *Biophys. J*. 2012, 102, 2192–2201.
[45] Bordignon E. Site-directed spin labeling of membrane proteins. *Top. Curr. Chem*. 2012, 321, 121–157.
[46] Madej MG, Soro SN, Kaback HR. Apo-intermediate in the transport cycle of lactose permease (LacY). *Proc. Natl. Acad. Sci. USA*. 2012, 109, E2970–2978.
[47] Sahu ID, McCarrick RM, Troxel KR, Zhang R, Smith HJ, Dunagan MM, Swartz MS, Rajan PV, Kroncke BM, Sanders CR, Lorigan GA. DEER EPR measurements for membrane protein structures via bifunctional spin labels and lipodisq nanoparticles. *Biochemistry*. 2013, 52, 6627–6632.
[48] Georgieva ER, Xiao S, Borbat PP, Freed JH, Eliezer D. Tau binds to membrane surfaces via short amphipatic helices located in its microtubule-binding repeats. *Biophys. J*. 2014, 107, 1–12.
[49] Mullen A, Hall J, Diegel J, Hassan I, Fey A, MacMillan F. Membrane transporters studied by EPR spectroscopy: structure determination and elucidation of functional dynamics. *Biochem. Soc. Trans*. 2016, 44, 905–915.
[50] Jeschke G. Ensemble models of proteins and protein domains based on distance distribution restraints. *Proteins*. 2016, 84, 544–560.
[51] Georgieva ER, Borbat PP, Norman HD, Freed JH. Mechanism of influenza A M2 transmembrane domain assembly in lipid membranes. *Sci. Rep*. 2015, 5, 11757.
[52] Claxton DP, Kazmier K, Mishra S, Mchaourab HS. Navigating membrane protein structure, dynamics, and energy landscapes using spin labeling and EPR spectroscopy. *Methods Enzymol*. 2015, 564, 349–387.
[53] Klare JP, Steinhoff HJ. Spin labeling studies of transmembrane signaling and transport: applications to phototaxis, ABC transporters and symporters. *Methods Enzymol*. 2015, 564, 315–347.
[54] Li Q, Shen R, Treger JS, Wanderling SS, Milewski W, Siwowska K, Bezanilla F, Perozo E. Resting state of the human proton channel dimer in a lipid bilayer. *Proc. Natl. Acad. Sci. USA*. 2015, 112, E5926–E5935.
[55] Kinde MN, Chen Q, Lawless MJ, Mowrey DD, Xu J, Saxena S, Xu Y, Tang P. Conformational changes underlying desensitization of the pentameric ligand-gated ion channel ELIC. *Structure*. 2015, 23, 995–1004.
[56] Georgieva ER, Borbat PP, Grushin K, Stoilova-McPhie S, Kulkarni NJ, Liang Z, Freed JH. Conformational response of influenza A M2 transmembrane domain to amantadine drug binding at low pH (pH 5.5). *Front. Physiol*. 2016, 7, 317.
[57] Georgieva ER, Borbat PP, Ginter C, Freed JH, Boudker O. Conformational ensemble of the sodium-coupled aspartate transporter. *Nat. Struct. Mol. Biol*. 2013, 20, 215–221.
[58] Dunkel S, Pulagam LP, Steinhoff HJ, Klare JP. In vivo EPR on spin labeled colicin A reveals an oligomeric assembly of the pore-forming domain in *E. coli* membranes. *Phys. Chem. Chem. Phys*. 2015, 17, 4875–4878.
[59] Joseph B, Sikora A, Bordignon E, Jeschke G, Cafiso DS, Prisner TF. Distance measurement on an endogenous membrane transporter in *E. coli* cells and native membranes using EPR spectroscopy. *Angew. Chem. Int. Ed. Engl*. 2015, 54, 6196–6199.
[60] Joseph B, Sikora A, Cafiso DS. Ligand induced conformational changes of a membrane transporter in *E. coli* cells observed with DEER/PELDOR. *J. Am. Chem. Soc*. 2016, 138, 1844–1847.
[61] Herget M, Baldauf C, Scholz C, Parcej D, Wiesmuller KH, Tampe R, Abele R, Bordignon E. Conformation of peptides bound to the transporter associated with antigen processing (TAP). *Proc. Natl. Acad. Sci. USA*. 2011, 108, 1349–1354.
[62] Klare JP, Steinhoff HJ. Spin labeling EPR. *Photosynth. Res*. 2009, 102, 377–390.
[63] Bleicken S, Jeschke G, Stegmueller C, Salvador-Gallego R, Garcia-Saez AJ, Bordignon E. Structural model of active Bax at the membrane. *Mol. Cell*. 2014, 56, 496–505.
[64] Lu B, Kiessling V, Tamm LK, Cafiso DS. The juxtamembrane linker of full-length synaptotagmin 1 controls oligomerization and calcium-dependent membrane binding. *J. Biol. Chem*. 2014, 289, 22161–22171.
[65] Tong J, Borbat PP, Freed JH, Shin YK. A scissors mechanism for stimulation of SNARE-mediated lipid mixing by cholesterol. *Proc. Natl. Acad. Sci. USA*. 2009, 106, 5141–5146.
[66] Schredelseker J, Paz A, Lopez CJ, Altenbach C, Leung CS, Drexler MK, Chen JN, Hubbell WL, Abramson J. High resolution structure and double electron-electron resonance of the zebrafish voltage-dependent anion channel 2 reveal an oligomeric population. *J. Biol. Chem*. 2014, 289, 12566–12577.
[67] Ambroso MR, Hegde BG, Langen R. Endophilin A1 induces different membrane shapes using a conformational switch that is regulated by phosphorylation. *Proc. Natl. Acad. Sci. USA*. 2014, 111, 6982–6987.
[68] Georgieva ER, Ramlall TF, Borbat PP, Freed JH, Eliezer D. Membrane-bound alpha-synuclein forms an extended helix: long-distance pulsed ESR measurements using vesicles, bicelles, and rodlike micelles. *J. Am. Chem. Soc*. 2008, 130, 12856–12857.
[69] Georgieva ER, Ramlall TF, Borbat PP, Freed JH, Eliezer D. The lipid-binding domain of wild type and mutant alpha-synuclein: compactness and interconversion between the broken and extended helix forms. *J. Biol. Chem*. 2010, 285, 28261–28274.
[70] Joseph B, Jeschke G, Goetz BA, Locher KP, Bordignon E. Transmembrane gate movements in the type II ATP-binding cassette (ABC) importer BtuCD-F during nucleotide cycle. *J. Biol. Chem*. 2011, 286, 41008–41017.

[71] Middleton DA, Reid DG, Watts A. The conformations of a functional spin-labeled derivative of gastric H/K-ATPase investigated by EPR spectroscopy. *Biochemistry*. 1995, 34, 7420–7429.
[72] Mittal A, Bohm S, Grutter MG, Bordignon E, Seeger MA. Asymmetry in the homodimeric ABC transporter MsbA recognized by a DARPin. *J. Biol. Chem*. 2012, 287, 20395–20406.
[73] Nicklisch SC, Wunnicke D, Borovykh IV, Morbach S, Klare JP, Steinhoff HJ, Kramer R. Conformational changes of the betaine transporter BetP from *Corynebacterium glutamicum* studied by pulse EPR spectroscopy. *Biochim. Biophys. Acta*. 2012, 1818, 359–366.
[74] Smirnova I, Kasho V, Choe JY, Altenbach C, Hubbell WL, Kaback HR. Sugar binding induces an outward facing conformation of LacY. *Proc. Natl. Acad. Sci. USA*. 2007, 104, 16504–16509.
[75] Borbat PP, Freed JH. Measuring distances by pulsed dipolar ESR spectroscopy: spin-labeled histidine kinases. *Methods Enzymol*. 2007, 423, 52–116.
[76] Borbat PP, Freed JH. Pros and cons of pulse dipolar ESR: DQC and DEER. *EPR Newsletter*. 2007, 17, 21–33.
[77] Jeschke G. DEER distance measurements on proteins. *Annu. Rev. Phys. Chem*. 2012, 63, 419–446.
[78] Cafiso DS. Taking the pulse of protein interactions by EPR spectroscopy. *Biophys. J*. 2012, 103, 2047–2048.
[79] Feintuch A, Otting G, Goldfarb D. Gd(3)(+) Spin labeling for measuring distances in biomacromolecules: why and how? *Methods Enzymol*. 2015, 563, 415–457.
[80] Hubbell WL, Cafiso DS, Altenbach C. Identifying conformational changes with site-directed spin labeling. *Nat. Struct. Biol*. 2000, 7, 735–739.
[81] Pulagam LP, Steinhoff HJ. Acidic pH-induced membrane insertion of colicin A into *E. coli* natural lipids probed by site-directed spin labeling. *J. Mol. Biol*. 2013, 425, 1782–1794.
[82] Cymer F, von Heijne G, White SH. Mechanisms of integral membrane protein insertion and folding. *J. Mol. Biol*. 2015, 427, 999–1022.
[83] Hubbell WL, McHaourab HS, Altenbach C, Lietzow MA. Watching proteins move using site-directed spin labeling. *Structure*. 1996, 4, 779–783.
[84] Zhang Z, Fleissner MR, Tipikin DS, Liang Z, Moscicki JK, Earle KA, Hubbell WL, Freed JH. Multifrequency electron spin resonance study of the dynamics of spin labeled T4 lysozyme. *J. Phys. Chem. B*. 2010, 114, 5503–5521.
[85] Steed PR, Zou P, Trone KE, Mchaourab HS. Structure and pH-induced structural rearrangements of the putative multidrug efflux pump EmrD in liposomes probed by site-directed spin labeling. *Biochemistry*. 2013, 52, 7964–7974.
[86] Pirman NL, Milshteyn E, Galiano L, Hewlett JC, Fanucci GE. Characterization of the disordered-to-alpha-helical transition of IA(3) by SDSL-EPR spectroscopy. *Protein Sci*. 2011, 20, 150–159.
[87] Belle V, Rouger S, Costanzo S, Liquiere E, Strancar J, Guigliarelli B, Fournel A, Longhi S. Mapping alpha-helical induced folding within the intrinsically disordered C-terminal domain of the measles virus nucleoprotein by site-directed spin-labeling EPR spectroscopy. *Proteins*. 2008, 73, 973–988.
[88] Mchaourab HS, Lietzow MA, Hideg K, Hubbell WL. Motion of spin-labeled side chains in T4 lysozyme. Correlation with protein structure and dynamics. *Biochemistry*. 1996, 35, 7692–7704.
[89] Budil DE, Lee S, Saxena S, Freed JH. Nonlinear-least-squares analysis of slow-motion EPR spectra in one and two dimentions using a modified Levenberg-Marquard algorithm. *J. Magn. Reson*. 1996, 120, 155–189.
[90] Freed JH. New technologies in electron spin resonance. *Annu. Rev. Phys. Chem.* 2000, 51, 655–689.
[91] Altenbach C, Greenhalgh DA, Khorana HG, Hubbell WL. A collision gradient method to determine the immersion depth of nitroxides in lipid bilayers: application to spin-labeled mutants of bacteriorhodopsin. *Proc. Natl. Acad. Sci. USA*. 1994, 91, 1667–1671.
[92] Altenbach C, Froncisz W, Hemker R, Mchaourab H, Hubbell WL. Accessibility of nitroxide side chains: absolute Heisenberg exchange rates from power saturation EPR. *Biophys. J*. 2005, 89, 2103–2112.
[93] Milov AD, Salikhov KM, Shirov MD. Application of ELDOR in electron-spin echo for paramagnetic centar space distributions in solids. *Fiz. Tverd. Tela. (Leningrad)*. 1981, 23, 075–982.
[94] Milov AD, Ponomarev AB, Tsvetkov YD. Electron electron double-resonance in electron-spin echo-model biradical systems and the sensitized photolysis of decalin. *Chem. Phys. Lett.* 1984, 110, 67–72.
[95] Jeschke G. Distance measurements in the nanometer range by pulse EPR. *Chemphyschem*. 2002, 3, 927–932.
[96] Jeschke G, Polyhach Y. Distance measurements on spin-labelled biomacromolecules by pulsed electron paramagnetic resonance. *Phys. Chem. Chem. Phys*. 2007, 9, 1895–1910.
[97] Pannier M, Veit S, Godt A, Jeschke G, Spiess HW. Dead-time free measurement of dipole-dipole interactions between electron spins. 2000. *J. Magn. Reson*. 2011, 213, 316–325.
[98] Borbat PP, Georgieva ER, Freed JH. Improved sensitivity for long-distance measurements in biomolecules: five-pulse double electron-electron resonance. *J. Phys. Chem. Lett*. 2013, 4, 170–175.
[99] Borbat PP, Mchaourab HS, Freed JH. Protein structure determination using long-distance constraints from double-quantum coherence ESR: study of T4 lysozyme. *J. Am. Chem. Soc*. 2002, 124, 5304–5314.
[100] Ruthstein S, Ji M, Shin BK, Saxena S. A simple double quantum coherence ESR sequence that minimizes nuclear modulations in Cu(2+)-ion based distance measurements. *J. Magn. Reson*. 2015, 257, 45–50.
[101] Kulik LV, Dzuba SA, Grigoryev IA, Tsvetkov YD. Electron dipole-dipole interaction in ESEEM of nitroxide biradicals. *Chem. Phys. Lett*. 2001, 343, 315–324.
[102] Milikisyants S, Scarpelli F, Finiguerra MG, Ubbink M, Huber M. A pulsed EPR method to determine distances between paramagnetic centers with strong spectral anisotropy and radicals: the dead-time free RIDME sequence. *J. Magn. Reson*. 2009, 201, 48–56.
[103] Collauto A, Frydman V, Lee MD, Abdelkader EH, Feintuch A, Swarbrick JD, Graham B, Otting G, Goldfarb D. RIDME distance measurements using Gd(iii) tags with a narrow central transition. *Phys. Chem. Chem. Phys*. 2016, 18, 19037–19049.
[104] Razzaghi S, Qi M, Nalepa AI, Godt A, Jeschke G, Savitsky A, Yulikov M. RIDME spectroscopy with Gd(III) centers. *J. Phys. Chem. Lett*. 2014, 5, 3970–3975.
[105] Astashkin AV. Mapping the structure of metalloproteins with RIDME. *Methods Enzymol*. 2015, 563, 251–284.

[106] Borbat PP, Freed JH. Double-quantum ESR and distance measurements. In *Distance Measurements in Biological Systems by EPR*, Berliner LJ, Eaton GR, Eaton SS, Eds., vol. 19, pp. 383–459, Kluwer Academic/Plenum Publishers: New York, 2000.
[107] Jeschke G, Pannier M, Godt A, Spiess HW. Dipolar spectroscopy and spin alignment in electron paramagnetic resonance. *Chem. Phys. Lett*. 2000, 331, 243–252.
[108] Chiang YW, Borbat PP, Freed JH. The determination of pair distance distributions by pulsed ESR using Tikhonov regularization. *J. Magn. Reson*. 2005, 172, 279–295.
[109] Polyhach Y, Stoll S, Jeschke G, Bordignon E. MMM molecular modeling software suite.
[110] Altenbach C. LongDistances Software.
[111] Chiang YW, Borbat PP, Freed JH. Maximum entropy: a complement to Tikhonov regularization for determination of pair distance distributions by pulsed ESR. *J. Magn. Reson*. 2005, 177, 184–196.
[112] Schiemann O, Prisner TF. Long-range distance determinations in biomacromolecules by EPR spectroscopy. *Q. Rev. Biophys*. 2007, 40, 1–53.
[113] Milov AD, Ponomarev AB, Tsvetkov YD. Modulation beats of signal of double electron-electron resonance in spin echo for biradical systems. *J. Struct. Chem*. 1984, 25, 710–713.
[114] Bode BE, Margraf D, Plackmeyer J, Durner G, Prisner TF, Schiemann O. Counting the monomers in nanometer-sized oligomers by pulsed electron-electron double resonance. *J. Am. Chem. Soc*. 2007, 129, 6736–6745.
[115] Jeschke G, Sajid M, Schulte M, Godt A. Three-spin correlations in double electron-electron resonance. *Phys. Chem. Chem. Phys*. 2009, 11, 6580–6591.
[116] Akbarzadeh A, Rezaei-Sadabady R, Davaran S, Joo SW, Zarghami N, Hanifehpour Y, Samiei M, Kouhi M, Nejati-Koshki K. Liposome: classification, preparation, and applications. *Nanoscale Res. Lett*. 2013, 8, 102.
[117] Allen TM. Liposomes. Opportunities in drug delivery. *Drugs*. 1997, 54 Suppl 4, 8–14.
[118] Mayer LD, Bally MB, Hope MJ, Cullis PR. Techniques for encapsulating bioactive agents into liposomes. *Chem. Phys. Lipids*. 1986, 40, 333–345.
[119] Kimelberg HK. Protein-liposome interactions and their relevance to the structure and function of cell membranes. *Mol. Cell. Biochem*. 1976, 10, 171–190.
[120] Ghosh S, Bell R. Liposomes. Applications in protein-lipid interaction studies. *Methods Mol. Biol*. 2002, 199, 49–60.
[121] Cantor RS. Lipid composition and the lateral pressure profile in bilayers. *Biophys. J*. 1999, 76, 2625–2639.
[122] Triba MN, Warschawski DE, Devaux PF. Reinvestigation by phosphorus NMR of lipid distribution in bicelles. *Biophys. J*. 2005, 88, 1887–1901.
[123] Sanders CR, 2nd, Schwonek JP. Characterization of magnetically orientable bilayers in mixtures of dihexanoylphosphatidylcholine and dimyristoylphosphatidylcholine by solid-state NMR. *Biochemistry*. 1992, 31, 8898–8905.
[124] Durr UH, Gildenberg M, Ramamoorthy A. The magic of bicelles lights up membrane protein structure. *Chem. Rev*. 2012, 112, 6054–6074.
[125] Liang B, Tamm LK. NMR as a tool to investigate the structure, dynamics and function of membrane proteins. *Nat. Struct. Mol. Biol*. 2016, 23, 468–474.
[126] Triba MN, Devaux PF, Warschawski DE. Effects of lipid chain length and unsaturation on bicelles stability. A phosphorus NMR study. *Biophys. J*. 2006, 91, 1357–1367.
[127] Huyton T, Pye VE, Briggs LC, Flynn TC, Beuron F, Kondo H, Ma J, Zhang X, Freemont PS. The crystal structure of murine p97/VCP at 3.6A. *J. Struct. Biol*. 2003, 144, 337–348.
[128] Wang H, Elferich J, Gouaux E. Structures of LeuT in bicelles define conformation and substrate binding in a membrane-like context. *Nat. Struct. Mol. Biol*. 2012, 19, 212–219.
[129] Hirva S, Jenusha P. Bicelles: a lipid nanostructure for transdermal delivery. *J. Crit. Rev*. 2016, 3, 17–22.
[130] Ward R, Pliotas C, Branigan E, Hacker C, Rasmussen A, Hagelueken G, Booth IR, Miller S, Lucocq J, Naismith JH, Schiemann O. Probing the structure of the mechanosensitive channel of small conductance in lipid bilayers with pulsed electron-electron double resonance. *Biophys. J*. 2014, 106, 834–842.
[131] Ghimire H, Abu-Baker S, Sahu ID, Zhou A, Mayo DJ, Lee RT, Lorigan GA. Probing the helical tilt and dynamic properties of membrane-bound phospholamban in magnetically aligned bicelles using electron paramagnetic resonance spectroscopy. *Biochim. Biophys. Acta*. 2012, 1818, 645–650.
[132] Bayburt TH, Grinkova YV, Sligar SG. Self-assembly of discoidal phospholipid bilayer nanoparticles with membrane scaffold proteins. *Nano Lett*. 2002, 2, 853–856.
[133] Denisov IG, Grinkova YV, Lazarides AA, Sligar SG. Directed self-assembly of monodisperse phospholipid bilayer nanodiscs with controlled size. *J. Am. Chem. Soc*. 2004, 126, 3477–3487.
[134] Orwick MC, Judge PJ, Procek J, Lindholm L, Graziadei A, Engel A, Grobner G, Watts A. Detergent-free formation and physicochemical characterization of nanosized lipid-polymer complexes: Lipodisq. *Angew. Chem. Int. Ed. Engl*. 2012, 51, 4653–4657.
[135] Orwick-Rydmark M, Lovett JE, Graziadei A, Lindholm L, Hicks MR, Watts A. Detergent-free incorporation of a seven-transmembrane receptor protein into nanosized bilayer lipodisq particles for functional and biophysical studies. *Nano Lett*. 2012, 12, 4687–4692.
[136] Zhang R, Sahu ID, Liu L, Osatuke A, Comer RG, Dabney-Smith C, Lorigan GA. Characterizing the structure of lipodisq nanoparticles for membrane protein spectroscopic studies. *Biochim. Biophys. Acta*. 2015, 1848, 329–333.
[137] Raschle T, Hiller S, Yu TY, Rice AJ, Walz T, Wagner G. Structural and functional characterization of the integral membrane protein VDAC-1 in lipid bilayer nanodiscs. *J. Am. Chem. Soc*. 2009, 131, 17777–17779.
[138] Ritchie TK, Kwon H, Atkins WM. Conformational analysis of human ATP-binding cassette transporter ABCB1 in lipid nanodiscs and inhibition by the antibodies MRK16 and UIC2. *J. Biol. Chem*. 2011, 286, 39489–39496.
[139] Rasmussen SG, Choi HJ, Fung JJ, Pardon E, Casarosa P, Chae PS, Devree BT, Rosenbaum DM, Thian FS, Kobilka TS, Schnapp A, Konetzki I, Sunahara RK, Gellman SH, Pautsch A, Steyaert J, Weis WI, Kobilka BK. Structure of a nanobody-stabilized active state of the beta(2) adrenoceptor. *Nature*. 2011, 469, 175–180.
[140] Efremov RG, Leitner A, Aebersold R, Raunser S. Architecture and conformational switch mechanism of the ryanodine receptor. *Nature*. 2015, 517, 39–43.

[141] Grushin K, Miller J, Dalm D, Stoilova-McPhie S. Factor VIII organisation on nanodiscs with different lipid composition. *Thromb. Haemost*. 2015, 113, 741–749.
[142] Zou P, McHaourab HS. Increased sensitivity and extended range of distance measurements in spin-labeled membrane proteins: Q-band double electron-electron resonance and nanoscale bilayers. *Biophys. J*. 2010, 98, L18–20.
[143] Alvarez FJ, Orelle C, Huang Y, Bajaj R, Everly RM, Klug CS, Davidson AL. Full engagement of liganded maltose-binding protein stabilizes a semi-open ATP-binding cassette dimer in the maltose transporter. *Mol. Microbiol*. 2015, 98, 878–894.
[144] Alvarez FJ, Orelle C, Davidson AL. Functional reconstitution of an ABC transporter in nanodiscs for use in electron paramagnetic resonance spectroscopy. *J. Am. Chem. Soc*. 2010, 132, 9513–9515.
[145] Martens C, Stein RA, Masureel M, Roth A, Mishra S, Dawaliby R, Konijnenberg A, Sobott F, Govaerts C, McHaourab HS. Lipids modulate the conformational dynamics of a secondary multidrug transporter. *Nat. Struct. Mol. Biol*. 2016, 23, 744–751.
[146] Andersson A, Maler L. Magnetic resonance investigations of lipid motion in isotropic bicelles. *Langmuir*. 2005, 21, 7702–7709.
[147] Snead D, Eliezer D. Alpha-synuclein function and dysfunction on cellular membranes. *Exp. Neurobiol*. 2014, 23, 292–313.
[148] Ottolini D, Cali T, Szabo I, Brini M. Alpha-synuclein at the intracellular and the extracellular side: functional and dysfunctional implications. *Biol. Chem*. 2017, 398, 77–100.
[149] Davidson WS, Jonas A, Clayton DF, George JM. Stabilization of alpha-synuclein secondary structure upon binding to synthetic membranes. *J. Biol. Chem*. 1998, 273, 9443–9449.
[150] Jo E, McLaurin J, Yip CM, St George-Hyslop P, Fraser PE. alpha-Synuclein membrane interactions and lipid specificity. *J. Biol. Chem*. 2000, 275, 34328–34334.
[151] Perrin RJ, Woods WS, Clayton DF, George JM. Interaction of human alpha-synuclein and Parkinson's disease variants with phospholipids. Structural analysis using site-directed mutagenesis. *J. Biol. Chem*. 2000, 275, 34393–34398.
[152] Ulmer TS, Bax A, Cole NB, Nussbaum RL. Structure and dynamics of micelle-bound human alpha-synuclein. *J. Biol. Chem*. 2005, 280, 9595–9603.
[153] Borbat P, Ramlall TF, Freed JH, Eliezer D. Inter-helix distances in lysophospholipid micelle-bound alpha-synuclein from pulsed ESR measurements. *J. Am. Chem. Soc*. 2006, 128, 10004–10005.
[154] Jao CC, Der-Sarkissian A, Chen J, Langen R. Structure of membrane-bound alpha-synuclein studied by site-directed spin labeling. *Proc. Natl. Acad. Sci. USA*. 2004, 101, 8331–8336.
[155] Jao CC, Hegde BG, Chen J, Haworth IS, Langen R. Structure of membrane-bound alpha-synuclein from site-directed spin labeling and computational refinement. *Proc. Natl. Acad. Sci. USA*. 2008, 105, 19666–19671.
[156] Bortolus M, Tombolato F, Tessari I, Bisaglia M, Mammi S, Bubacco L, Ferrarini A, Maniero AL. Broken helix in vesicle and micelle-bound alpha-synuclein: insights from site-directed spin labeling-EPR experiments and MD simulations. *J. Am. Chem. Soc*. 2008, 130, 6690–6691.
[157] Drescher M, van Rooijen BD, Veldhuis G, Subramaniam V, Huber M. A stable lipid-induced aggregate of alpha-synuclein. *J. Am. Chem. Soc*. 2010, 132, 4080–4082.
[158] Robotta M, Hintze C, Schildknecht S, Zijlstra N, Jungst C, Karreman C, Huber M, Leist M, Subramaniam V, Drescher M. Locally resolved membrane binding affinity of the N-terminus of alpha-synuclein. *Biochemistry*. 2012, 51, 3960–3962.
[159] Kumar P, Segers-Nolten IM, Schilderink N, Subramaniam V, Huber M. Parkinson's protein alpha-synuclein binds efficiently and with a novel conformation to two natural membrane mimics. *PLoS One*. 2015, 10, e0142795.
[160] Cleveland DW, Hwo SY, Kirschner MW. Purification of tau, a microtubule-associated protein that induces assembly of microtubules from purified tubulin. *J. Mol. Biol*. 1977, 116, 207–225.
[161] Cleveland DW, Hwo SY, Kirschner MW. Physical and chemical properties of purified tau factor and the role of tau in microtubule assembly. *J. Mol. Biol*. 1977, 116, 227–247.
[162] Brandt R, Leger J, Lee G. Interaction of tau with the neural plasma membrane mediated by tau's amino-terminal projection domain. *J. Cell. Biol*. 1995, 131, 1327–1340.
[163] Elbaum-Garfinkle S, Ramlall T, Rhoades E. The role of the lipid bilayer in tau aggregation. *Biophys. J*. 2010, 98, 2722–2730.
[164] Spillantini MG, Goedert M. Tau pathology and neurodegeneration. *Lancet Neurol*. 2013, 12, 609–622.
[165] Hanelt I, Wunnicke D, Bordignon E, Steinhoff HJ, Slotboom DJ. Conformational heterogeneity of the aspartate transporter Glt(Ph). *Nat. Struct. Mol. Biol*. 2013, 20, 210–214.
[166] Yernool D, Boudker O, Jin Y, Gouaux E. Structure of a glutamate transporter homologue from *Pyrococcus horikoshii*. *Nature* 2004, 431, 811–818.
[167] Boudker O, Ryan RM, Yernool D, Shimamoto K, Gouaux E. Coupling substrate and ion binding to extracellular gate of a sodium-dependent aspartate transporter. *Nature* 2007, 445, 387–393.
[168] Reyes N, Ginter C, Boudker O. Transport mechanism of a bacterial homologue of glutamate transporters. *Nature* 2009, 462, 880–885.
[169] Verdon G, Boudker O. Crystal structure of an asymmetric trimer of a bacterial glutamate transporter homolog. *Nat. Struct. Mol. Biol*. 2012, 19, 355–357.
[170] Focke PJ, Moenne-Loccoz P, Larsson HP. Opposite movement of the external gate of a glutamate transporter homolog upon binding cotransported sodium compared with substrate. *J. Neurosci*. 2011, 31, 6255–6262.
[171] Drew D, Boudker O. Shared molecular mechanisms of membrane transporters. *Annu. Rev. Biochem*. 2016, 85, 543–572.
[172] Tang S, Henne WM, Borbat PP, Buchkovich NJ, Freed JH, Mao Y, Fromme JC, Emr SD. Structural basis for activation, assembly and membrane binding of ESCRT-III Snf7 filaments. *Elife*. 2015, 4, e12548.
[173] Sugrue RJ, Hay AJ. Structural characteristics of the M2 protein of influenza A viruses: evidence that it forms a tetrameric channel. *Virology* 1991, 180, 617–624.

Bionote

Elka R. Georgieva
Department of Physiology and Biophysics, Weill Cornell Medicine, 1300 York Avenue, New York, NY 10065, USA,
erg2013@med.cornell.edu

Elka R. Georgieva is an Instructor in Physiology and Biophysics at Weill Cornell Medicine, New York, USA. She received her PhD from the Institute of Catalysis at the Bulgarian Academy of Sciences where she used electron paramagnetic resonance (EPR) spectroscopy to develop radiation dosimeters based on gamma irradiated saccharides. After completing her PhD, she joined the Department of Biochemistry and Biophysics, Stockholm University as a Postdoc to apply her EPR expertise in studies of radical-enzymes and to expand her knowledge in protein biochemistry and biophysics. Thereafter, E. Georgieva relocated to the Department of Chemistry and Chemical Biology, Cornell University, USA where she joined the National Biomedical Center for Advanced ESR Technology (ACERT) and worked for nearly eight and a half years studying the structure and function of a range of membrane proteins, including human alphasynuclein and tau, glutamate transporters, M2 proton channel from influenza A virus, and others. While at ACERT, E. Georgieva contributed significant research in the application of EPR method and spin-labeling to solve critical biomedical problems. She has been a co-investigator and a key contributor in several strategic projects establishing novel mechanisms of protein physiology and malfunction. Her current scientific focus is on the utilizing and developing biophysical and biochemical approaches to study at the nanoscale level the pathways of viral infectivity and proliferation, and to learn how viruses modify the host cell homeostasis. She is also interested in molecular mechanisms related to nerve cells function.